



# Silicon containing new salicylaldimine Pd(II) and Co(II) metal complexes as efficient catalysts in transformation of carbon dioxide (CO<sub>2</sub>) to cyclic carbonates

Mahmut Ulusoy<sup>a,\*\*</sup>, Ahmet Kilic<sup>a,\*</sup>, Mustafa Durgun<sup>a</sup>, Zeynep Tasci<sup>b</sup>, Bekir Cetinkaya<sup>b</sup>

<sup>a</sup> Department of Chemistry, University of Harran, 63190 Sanliurfa, Turkey

<sup>b</sup> Department of Chemistry, Ege University, 35100 Bornova, Izmir, Turkey

## ARTICLE INFO

### Article history:

Received 29 November 2010

Received in revised form

3 January 2011

Accepted 3 January 2011

### Keywords:

Pd(II) complex

Catalyst

Carbon dioxide

Salicylaldimine

Cyclic carbonate

## ABSTRACT

A new series of metal complexes of salicylaldimine ligands with Pd(II) and Co(II) have been prepared and characterized by different techniques (elemental analysis, UV–vis, FT-IR, <sup>1</sup>H NMR spectra, magnetic susceptibility measurements). Electronic spectra and magnetic susceptibility measurements reveal square planar geometry for Pd(II) metal complex and tetrahedral geometry for Co(II) metal complex. The synthesized Pd(II) and Co(II) complexes were also tested as catalysts for the formation of cyclic organic carbonates from carbon dioxide and liquid epoxides which served as both reactant and solvent. The results showed that the [M(L<sub>3</sub>)<sub>2</sub>] (M = Pd or Co) complexes bearing 5-methyl substitution on the aryl ring are more efficient than the other Pd(II) and Co(II) metal complexes for the formation of cyclic organic carbonates from carbon dioxide. These catalysts, [Pd(L<sub>3</sub>)<sub>2</sub>] and [Co(L<sub>3</sub>)<sub>2</sub>] complexes and location (*p*-position of phenoxy) of electron donating methyl substituent in particular, effectively promote the of carbon dioxide activation with liquid epoxides under solvent-free homogeneous conditions. Furthermore, [Pd(L<sub>3</sub>)<sub>2</sub>] can be reused more than eight times with a minimal loss of its original catalytic activities.

© 2011 Elsevier B.V. All rights reserved.

## 1. Introduction

In the current global climate, with high oil prices, increasing concern over global warming, and depleting petroleum resources, the development of renewable carbon sources is of the utmost importance. Carbon dioxide (CO<sub>2</sub>) is a particularly attractive alternative feedstock as it is inexpensive, highly naturally abundant, and the by-product of many industrial processes, including combustion [1]. Also, utilizing renewable resources is a prerequisite for a sustainable society. One easily available renewable carbon resource is carbon dioxide (CO<sub>2</sub>), which has the advantages of being nontoxic, abundant and economical. Carbon dioxide (CO<sub>2</sub>) is also attractive as an environmentally friendly chemical reagent and is especially useful as a phosgene substitute [2]. Carbon dioxide fixation has received much attention in last decades since carbon dioxide is the most inexpensive and infinite carbon resource [3,4]. The cyclic carbonates are one kind of carbon dioxide fixation products and widely used as monomer for polymer synthesis, an aprotic solvent, a pharmaceutical intermediate [3–7]. The synthesis

of cyclic carbonate includes three aspects: catalytic reaction of CO<sub>2</sub> and epoxide, electrochemical reaction of CO<sub>2</sub> and epoxide, and oxidative carboxylation of olefin. Various catalysts systems were developed for the coupling carbon dioxide and epoxides in the so-called carbon dioxide fixation process, including porphyrin, phthalocyanine, salen metal complexes, metal oxides, zeolite, nanogold, alkali metal salts, ionic liquid, and so on [3].

Cyclic carbonates are used industrially as polar aprotic solvents, substrates for small molecule synthesis, additives, antifoam agents for antifreeze, and plasticizers [8,9]. The five-membered ring cyclic carbonates (1,3-dioxolan-2-ones) are generally incapable of ring-opening polymerization due to their thermodynamic stability, but do undergo polymerization with partial loss of CO<sub>2</sub> to yield macromolecules with both ether and carbonate linkages [10]. Due to such uses, a number of syntheses of cyclic carbonates have been described over the last 30 years. For example, tetraalkylammonium salts, phosphanes, main-group and transition-metal complexes, and alkali metals convert epoxides and CO<sub>2</sub> to cyclic carbonates [11]. As observed in early studies, only a few metals are active for the coupling of epoxides and CO<sub>2</sub>, including Al, Cr, Co, Mg, Li, Zn, Cu, and Cd [12,13,19]. Studies have shown that large differences in catalytic efficacy result from the organic frameworks surrounding these metals. Accordingly, subsequent studies have largely focused on empirical modification of ligands to generate improved catalysts. To the best of our knowledge, Schiff bases containing Pd(II) as

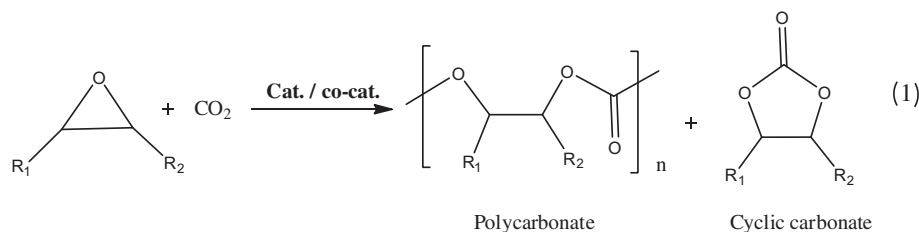
\* Corresponding author. Tel.: +90 414 318 3587; fax: +90 414 318 3541.

\*\* Corresponding author. Tel.: +90 414 318 3000/1267; fax: +90 414 318 3541.

E-mail addresses: [ulusoymahmut@harran.edu.tr](mailto:ulusoymahmut@harran.edu.tr) (M. Ulusoy), [kilica63@harran.edu.tr](mailto:kilica63@harran.edu.tr) (A. Kilic).

the metal centre have not been used as catalysts for chemical fixation of carbon dioxide.

room temperature. The crystals were filtered in vacuum. Then the products were recrystallized from hot ethanol.



Darensbourg and others noted that coupling of epoxides and carbon dioxide produced either corresponding cyclic carbonates or polycarbonates depending on the nature of epoxide, the metal catalyst and the reaction conditions such as temperature and pressure [14–20] (Eq. (1)).

The development of efficient recoverable and reusable catalysts that can be easily prepared, recovered and reused without losing their activities has received much attention from a practical and environmental point of view [21]. In this study, four salicylaldimine ligands and their Pd(II) and Co(II) metal complexes have been synthesized and characterized by elemental analysis, UV–vis, FT-IR,  $^1\text{H}$  NMR spectra, and magnetic susceptibility measurements. We firstly reported novel and efficient catalysts of silicon-containing Pd(II) and Co(II) Schiff base complexes in conjunction with 4-dimethylamino-pyridine (DMAP) for the conversion of  $\text{CO}_2$  to cyclic carbonates.

## 2. Experimental

All reagents and solvents were of reagent-grade quality and obtained from commercial suppliers. Elemental analysis was carried out on a LECO CHNS model 932 elemental analyzer. FT-IR spectra were recorded on a Perkin Elmer Spectrum RXI FT-IR spectrometer as KBr pellets.  $^1\text{H}$  NMR spectra were recorded at 297 K using a Varian AS-400 MHz spectrometer. UV–vis spectra were recorded on a Perkin Elmer Lambda 25 PC UV–Vis spectrometer. Melting points were measured in open capillary tubes with a Stuart Scientific melting point apparatus and uncorrected. Magnetic susceptibilities were determined on a Sherwood Scientific Magnetic Susceptibility Balance (Model MK1) at room temperature (20 °C) using  $\text{Hg}[\text{Co}(\text{SCN})_4]$  as a calibrant; diamagnetic corrections were calculated from Pascal's constants [22–24]. Catalytic tests performed in a PARR 4843 50 mL stainless steel pressure reactor.

### 2.1. Synthesis of the ligands ( $L_1\text{H}$ , $L_2\text{H}$ , $L_3\text{H}$ and $L_4\text{H}$ )

$N$ -[ $N$ -(3-(trimethoxysilyl)propyl)-ethylenediamine]-3-methylsalicylaldimine ( $L_1\text{H}$ ),  $N$ -[ $N$ -(3-(trimethoxysilyl)propyl)-ethylenediamine]-4-methoxysalicylaldimine ( $L_2\text{H}$ ),  $N$ -[ $N$ -(3-(trimethoxysilyl)propyl)-ethylenediamine]-5-methylsalicylaldimine ( $L_3\text{H}$ ) and  $N$ -[ $N$ -(3-(trimethoxysilyl)propyl)-ethylenediamine]-5-methoxysalicylaldimine ( $L_4\text{H}$ ) ligands were synthesized by the reaction of 5.0 mmol (1.11 g)  $N$ -(3-(trimethoxysilyl)propyl)-ethylenediamine in 50 ml absolute ethanol and 5.0 mmol (0.68 g) 3-methylsalicylaldehyde for ( $L_1\text{H}$ ), 5.0 mmol (0.76 g) 4-methoxysalicylaldehyde for ( $L_2\text{H}$ ), 5.0 mmol (0.68 g) 5-methylsalicylaldehyde for ( $L_3\text{H}$ ) and 5.0 mmol (0.76 g) 5-methoxysalicylaldehyde for ( $L_4\text{H}$ ), in 30 ml absolute ethanol. Also, 3–4 drops of formic acid was added as catalyst. The mixtures were refluxed for 6 h, followed by cooling to

#### 2.1.1. For ( $L_1\text{H}$ ) ligand

Color: yellow; m.p: 220 °C; yield (%): 85. Anal. Calc. for  $\text{C}_{16}\text{H}_{28}\text{N}_2\text{O}_4\text{Si}$  (F.W: 340.5 g/mol): C, 56.44; H, 8.29; N, 8.23. Found: C, 56.28; H, 8.38; N, 8.14%.  $^1\text{H}$  NMR (400 MHz, DMSO,  $\text{Me}_4\text{Si}$ , ppm):  $\delta = 13.66$  (s, 1H,  $-\text{OH}$ , D-exchangeable),  $\delta = 8.60$  (s, 1H,  $\text{NH}$ ),  $\delta = 8.17$  (s, 1H,  $\text{HC}=\text{N}$ ),  $\delta = 7.25$ – $7.20$  (m, 2H,  $\text{Ar}-\text{CH}$ ),  $\delta = 6.81$ – $6.77$  (m, 1H,  $\text{Ar}-\text{CH}$ ),  $\delta = 3.93$  (s, 9H,  $\text{O}-\text{CH}_3$ ),  $\delta = 2.51$ – $2.49$  (m, 8H,  $\text{C}-\text{CH}_2$ ),  $\delta = 2.15$  (s, 3H,  $\text{C}-\text{CH}_3$ ) and  $\delta = 1.91$  (s, 2H,  $\text{Si}-\text{CH}_2$ ). IR (KBr pellets,  $\nu_{\text{max}}/\text{cm}^{-1}$ ): 3520–2504  $\nu(\text{OH})$ , 3054  $\nu(\text{Ar}-\text{CH})$ , 2946–2705  $\nu(\text{Alif}-\text{CH})$ , 1631  $\nu(\text{C}=\text{N})$ , 1493–1348  $\nu(\text{C}=\text{C})$ , 1264  $\nu(\text{C}-\text{O})$  and 1128–1087  $\nu(\text{Si}-\text{O})$ . UV–vis ( $\lambda_{\text{max}}$ , nm, \* = shoulder peak): 260, 325, 424\* (in EtOH), 264, 322, 403\* (in MeOH) and 268, 322 (in DMF).

#### 2.1.2. For ( $L_2\text{H}$ ) ligand

Color: yellow; m.p: 260 °C; yield (%): 83. Anal. Calc. for  $\text{C}_{16}\text{H}_{28}\text{N}_2\text{O}_5\text{Si}$  (F.W: 356.5 g/mol): C, 53.91; H, 7.92; N, 7.86. Found: C, 53.76; H, 7.85; N, 7.91%.  $^1\text{H}$  NMR (400 MHz, DMSO,  $\text{Me}_4\text{Si}$ , ppm):  $\delta = 13.34$  (s, 1H,  $-\text{OH}$ , D-exchangeable),  $\delta = 8.42$  (s, 1H,  $\text{NH}$ ),  $\delta = 8.19$  (s, 1H,  $\text{HC}=\text{N}$ ),  $\delta = 7.27$ – $7.25$  (d, 1H,  $J = 8.8$  Hz,  $\text{Ar}-\text{CH}$ ),  $\delta = 6.40$ – $6.37$  (m, 1H,  $\text{Ar}-\text{CH}$ ),  $\delta = 6.32$  (d, 1H,  $J = 2.4$  Hz,  $\text{Ar}-\text{CH}$ ),  $\delta = 3.82$  (s, 3H,  $\text{Si}-\text{O}-\text{CH}_3$ ),  $\delta = 3.74$  (s, 9H,  $\text{O}-\text{CH}_3$ ),  $\delta = 2.51$ – $2.49$  (m, 6H,  $\text{C}-\text{CH}_2$ ),  $\delta = 1.90$  (s, 2H,  $\text{C}-\text{CH}_2$ ) and  $\delta = 1.23$  (s, 2H,  $\text{Si}-\text{CH}_2$ ). IR (KBr pellets,  $\nu_{\text{max}}/\text{cm}^{-1}$ ): 3534–2545  $\nu(\text{OH})$ , 3060  $\nu(\text{Ar}-\text{CH})$ , 2937–2764  $\nu(\text{Alif}-\text{CH})$ , 1631  $\nu(\text{C}=\text{N})$ , 1494–1345  $\nu(\text{C}=\text{C})$ , 1276  $\nu(\text{C}-\text{O})$  and 1116–1025  $\nu(\text{Si}-\text{O})$ . UV–vis ( $\lambda_{\text{max}}$ , nm, \* = shoulder peak): 278, 305\*, 378, 427\* (in EtOH), 252, 280, 301, 379\* (in MeOH) and 278, 306, 383\* (in DMF).

#### 2.1.3. For ( $L_3\text{H}$ ) ligand

Color: yellow; m.p: 230 °C; yield (%): 84. Anal. Calc. for  $\text{C}_{16}\text{H}_{28}\text{N}_2\text{O}_4\text{Si}$  (F.W: 340.5 g/mol): C, 56.44; H, 8.29; N, 8.23. Found: C, 56.38; H, 8.32; N, 8.42%.  $^1\text{H}$  NMR (400 MHz, DMSO,  $\text{Me}_4\text{Si}$ , ppm):  $\delta = 13.08$  (s, 1H,  $-\text{OH}$ , D-exchangeable),  $\delta = 8.50$  (s, 1H,  $\text{NH}$ ),  $\delta = 8.19$  (s, 1H,  $\text{HC}=\text{N}$ ),  $\delta = 7.19$  (s, 1H,  $\text{Ar}-\text{CH}$ ),  $\delta = 7.12$ – $7.10$  (d, 1H,  $J = 8.8$  Hz,  $\text{Ar}-\text{CH}$ ),  $\delta = 6.75$ – $6.73$  (d, 1H,  $J = 8.8$  Hz,  $\text{Ar}-\text{CH}$ ),  $\delta = 3.88$  (s, 9H,  $\text{O}-\text{CH}_3$ ),  $\delta = 2.49$ – $2.48$  (m, 8H,  $\text{C}-\text{CH}_2$ ),  $\delta = 2.03$  (s, 3H,  $\text{C}-\text{CH}_3$ ) and  $\delta = 1.22$  (s, 2H,  $\text{Si}-\text{CH}_2$ ). IR (KBr pellets,  $\nu_{\text{max}}/\text{cm}^{-1}$ ): 3546–2574  $\nu(\text{OH})$ , 3019  $\nu(\text{Ar}-\text{CH})$ , 2938–2797  $\nu(\text{Alif}-\text{CH})$ , 1632  $\nu(\text{C}=\text{N})$ , 1493–1347  $\nu(\text{C}=\text{C})$ , 1280  $\nu(\text{C}-\text{O})$  and 1134–1040  $\nu(\text{Si}-\text{O})$ . UV–vis ( $\lambda_{\text{max}}$ , nm, \* = shoulder peak): 259, 334 (in EtOH), 263, 327, 413\* (in MeOH) and 262, 326 (in DMF).

#### 2.1.4. For ( $L_4\text{H}$ ) ligand

Color: yellow; m.p: 225 °C; yield (%): 88. Anal. Calc. for  $\text{C}_{16}\text{H}_{28}\text{N}_2\text{O}_5\text{Si}$  (F.W: 356.5 g/mol): C, 53.91; H, 7.92; N, 7.86. Found: C, 53.78; H, 7.86; N, 7.71%.  $^1\text{H}$  NMR (400 MHz, DMSO,  $\text{Me}_4\text{Si}$ , ppm):  $\delta = 12.68$  (s, 1H,  $-\text{OH}$ , D-exchangeable),  $\delta = 8.53$  (s, 1H,  $\text{NH}$ ),  $\delta = 8.15$  (s, 1H,  $\text{HC}=\text{N}$ ),  $\delta = 7.00$  (s, 1H,  $\text{Ar}-\text{CH}$ ),  $\delta = 6.93$ – $6.90$  (m, 1H,  $\text{Ar}-\text{CH}$ ),  $\delta = 6.79$ – $6.77$  (d, 1H,  $J = 8.4$  Hz,  $\text{Ar}-\text{CH}$ ),  $\delta = 3.89$  (s, 3H,

Si–O–CH<sub>3</sub>,  $\delta = 3.68$  (s, 9H, O–CH<sub>3</sub>),  $\delta = 2.49$ – $2.47$  (m, 6H, C–CH<sub>2</sub>),  $\delta = 1.89$  (s, 2H, C–CH<sub>2</sub>) and  $\delta = 1.21$  (s, 2H, Si–CH<sub>2</sub>). IR (KBr pellets,  $\nu_{\max}/\text{cm}^{-1}$ ): 3517–2533  $\nu(\text{OH})$ , 3048  $\nu(\text{Ar–CH})$ , 2936–2746  $\nu(\text{Alif–CH})$ , 1632  $\nu(\text{C=N})$ , 1494–1347  $\nu(\text{C=C})$ , 1273  $\nu(\text{C–O})$  and 1158–1032  $\nu(\text{Si–O})$ . UV–vis ( $\lambda_{\max}$ , nm, \* = shoulder peak): 258, 352 445\* (in EtOH), 264, 343, 456\* (in MeOH) and 268, 344 (in DMF).

## 2.2. Synthesis of the Pd(II) and Co(II) metal complexes

The metal(II) complexes were prepared by the same general method: L<sub>1</sub>H (0.34 g, 1.0 mmol), L<sub>2</sub>H (0.36 g, 1.0 mmol), L<sub>3</sub>H (0.34 g, 1.0 mmol) and L<sub>4</sub>H (0.36 g, 1.0 mmol) were dissolved in 40 ml methanol at room temperature. The suspended solution of the [Pd(Ac)<sub>2</sub>] (0.11 g, 0.5 mmol) or [Co(Ac)<sub>2</sub>·4H<sub>2</sub>O] (0.13 g, 0.5 mmol) in 20 ml in methanol was added under a nitrogen atmosphere with continuous stirring. The stirred mixtures were then heated to the reflux temperature for 8 h and were maintained at this temperature. Then, the mixture was evaporated to a volume of 10 ml under vacuum and left to cool to room temperature. The precipitated compounds were filtered in vacuum. The crude products were dissolved in chloroform and filtered via cannula. Then the products were recrystallized from chloroform–ethanol.

### 2.2.1. For [Pd(L<sub>1</sub>)<sub>2</sub>]

Color: green; m.p.: >300 °C; yield (%): 76. Anal. Calc. for C<sub>32</sub>H<sub>54</sub>N<sub>4</sub>O<sub>8</sub>Si<sub>2</sub>Pd (F.W: 785 g/mol): C, 48.94; H, 6.93; N, 7.13. Found: C, 48.79; H, 6.98; N, 7.06%. <sup>1</sup>H NMR (400 MHz, DMSO, Me<sub>4</sub>Si, ppm):  $\delta = 8.52$  (s, 2H, NH),  $\delta = 8.16$  (s, 2H, HC=N),  $\delta = 7.23$ – $7.19$  (m, 4H, Ar–CH),  $\delta = 6.82$  (s, 2H, Ar–CH),  $\delta = 3.96$  (s, 18H, O–CH<sub>3</sub>),  $\delta = 2.49$ – $2.46$  (m, 16H, C–CH<sub>2</sub>),  $\delta = 2.11$  (s, 6H, C–CH<sub>3</sub>) and  $\delta = 1.86$  (s, 4H, Si–CH<sub>2</sub>). IR (KBr pellets,  $\nu_{\max}/\text{cm}^{-1}$ ): 3042  $\nu(\text{Ar–CH})$ , 2939–2805  $\nu(\text{Alif–CH})$ , 1602  $\nu(\text{C=N})$ , 1455–1361  $\nu(\text{C=C})$ , 1282  $\nu(\text{C–O})$ , 1135–1023  $\nu(\text{Si–O})$ , 515  $\nu(\text{Pd–N})$  and 462  $\nu(\text{Pd–O})$ . UV–vis ( $\lambda_{\max}$ , nm, \* = shoulder peak): 268, 334, 408, 502\* (in MeOH) and 266, 328 (in DMF).

### 2.2.2. For [Pd(L<sub>2</sub>)<sub>2</sub>]

Color: green; m.p.: >300 °C; yield (%): 78. Anal. Calc. for C<sub>32</sub>H<sub>54</sub>N<sub>4</sub>O<sub>10</sub>Si<sub>2</sub>Pd (F.W: 817 g/mol): C, 47.02; H, 6.66; N, 6.85. Found: C, 47.12; H, 6.59; N, 6.92%. <sup>1</sup>H NMR (400 MHz, DMSO, Me<sub>4</sub>Si, ppm):  $\delta = 8.58$  (s, 2H, NH),  $\delta = 8.13$  (s, 2H, HC=N),  $\delta = 7.62$ – $7.60$  (d, 2H, J = 8.8 Hz, Ar–CH),  $\delta = 7.28$ – $6.23$  (m, 2H, Ar–CH),  $\delta = 6.56$ – $6.19$  (m, 2H, Ar–CH),  $\delta = 3.79$  (s, 6H, Si–O–CH<sub>3</sub>),  $\delta = 3.72$  (s, 18H, O–CH<sub>3</sub>),  $\delta = 2.57$ – $2.52$  (m, 12H, C–CH<sub>2</sub>),  $\delta = 1.22$  (s, 4H, C–CH<sub>2</sub>) and  $\delta = 0.83$  (s, 4H, Si–CH<sub>2</sub>). IR (KBr pellets,  $\nu_{\max}/\text{cm}^{-1}$ ): 3042  $\nu(\text{Ar–CH})$ , 2936–2847  $\nu(\text{Alif–CH})$ , 1605  $\nu(\text{C=N})$ , 1456–1361  $\nu(\text{C=C})$ , 1290  $\nu(\text{C–O})$ , 1121–1023  $\nu(\text{Si–O})$ , 519  $\nu(\text{Pd–N})$ , 465  $\nu(\text{Pd–O})$ . UV–vis ( $\lambda_{\max}$ , nm, \* = shoulder peak): 278, 306\*, 376 (in MeOH) and 279, 306\*, 373, 514 (in DMF).

### 2.2.3. For [Pd(L<sub>3</sub>)<sub>2</sub>]

Color: green; m.p.: >300 °C; yield (%): 70. Anal. Calc. for C<sub>32</sub>H<sub>54</sub>N<sub>4</sub>O<sub>8</sub>Si<sub>2</sub>Pd (F.W: 785 g/mol): C, 48.94; H, 6.93; N, 7.13. Found: C, 48.81; H, 6.82; N, 7.18%. <sup>1</sup>H NMR (400 MHz, DMSO, Me<sub>4</sub>Si, ppm):  $\delta = 10.10$  (s, 2H, NH),  $\delta = 8.12$  (s, 2H, HC=N),  $\delta = 7.70$ – $7.69$  (d, 2H, J = 3.2 Hz, Ar–CH),  $\delta = 7.13$ – $6.92$  (m, 2H, Ar–CH),  $\delta = 6.74$ – $6.61$  (m, 2H, Ar–CH),  $\delta = 3.81$  (s, 18H, O–CH<sub>3</sub>),  $\delta = 2.48$ – $2.22$  (m, 18H, C–CH<sub>2</sub>),  $\delta = 2.12$  (s, 6H, C–CH<sub>3</sub>) and  $\delta = 1.09$  (s, 4H, Si–CH<sub>2</sub>). IR (KBr pellets,  $\nu_{\max}/\text{cm}^{-1}$ ): 3013  $\nu(\text{Ar–CH})$ , 2954–2859  $\nu(\text{Alif–CH})$ , 1603  $\nu(\text{C=N})$ , 1493–1381  $\nu(\text{C=C})$ , 1285  $\nu(\text{C–O})$ , 1123–1039  $\nu(\text{Si–O})$ , 512  $\nu(\text{Pd–N})$ , 467  $\nu(\text{Pd–O})$ . UV–vis ( $\lambda_{\max}$ , nm, \* = shoulder peak): 278, 323\*, 402, 514 (in MeOH) and 270, 318, 406 (in DMF).

### 2.2.4. For [Pd(L<sub>4</sub>)<sub>2</sub>]

Color: green; m.p.: >300 °C; yield (%): 73. Anal. Calc. for C<sub>32</sub>H<sub>54</sub>N<sub>4</sub>O<sub>10</sub>Si<sub>2</sub>Pd (F.W: 817 g/mol): C, 47.02; H, 6.66; N, 6.85. Found: C, 47.08; H, 6.58; N, 6.94%. <sup>1</sup>H NMR (400 MHz, DMSO, Me<sub>4</sub>Si, ppm):  $\delta = 10.12$  (s, 2H, NH),  $\delta = 8.06$  (s, 2H, HC=N),  $\delta = 7.71$ – $7.68$  (d, 2H, J = 12 Hz, Ar–CH),  $\delta = 7.12$ – $6.88$  (m, 2H, Ar–CH),  $\delta = 6.76$ – $6.74$  (d, 2H, J = 8.3 Hz, Ar–CH),  $\delta = 3.81$  (s, 6H, Si–O–CH<sub>3</sub>),  $\delta = 3.66$  (s, 18H, O–CH<sub>3</sub>),  $\delta = 2.48$ – $2.45$  (m, 12H, C–CH<sub>2</sub>),  $\delta = 1.22$  (s, 4H, C–CH<sub>2</sub>) and  $\delta = 0.83$ – $0.81$  (m, 4H, Si–CH<sub>2</sub>). IR (KBr pellets,  $\nu_{\max}/\text{cm}^{-1}$ ): 3052  $\nu(\text{Ar–CH})$ , 2958–2854  $\nu(\text{Alif–CH})$ , 1616  $\nu(\text{C=N})$ , 1489–1387  $\nu(\text{C=C})$ , 1287  $\nu(\text{C–O})$ , 1122–1039  $\nu(\text{Si–O})$ , 520  $\nu(\text{Pd–N})$ , 463  $\nu(\text{Pd–O})$ . UV–vis ( $\lambda_{\max}$ , nm, \* = shoulder peak): 275, 321\*, 413 (in MeOH) and 281, 330\*, 431 (in DMF).

### 2.2.5. For [Co(L<sub>1</sub>)<sub>2</sub>]

Color: dark brown; m.p.: >300 °C; yield (%): 68. Anal. Calc. for C<sub>32</sub>H<sub>54</sub>N<sub>4</sub>O<sub>8</sub>Si<sub>2</sub>Co (F.W: 770 g/mol): C, 52.09; H, 7.38; N, 7.59. Found: C, 52.16; H, 7.27; N, 7.64%. IR (KBr pellets,  $\nu_{\max}/\text{cm}^{-1}$ ): 3055  $\nu(\text{Ar–CH})$ , 2923–2871  $\nu(\text{Alif–CH})$ , 1612  $\nu(\text{C=N})$ , 1455–1397  $\nu(\text{C=C})$ , 1281  $\nu(\text{C–O})$ , 1124–1044  $\nu(\text{Si–O})$ , 516  $\nu(\text{Pd–N})$ , 468  $\nu(\text{Pd–O})$ .  $\mu_{\text{eff}} = 2.24$  [B.M.]. UV–vis ( $\lambda_{\max}$ , nm, \* = shoulder peak): 264, 301, 396, 639 (in MeOH) and 268, 392 (in DMF).

### 2.2.6. For [Co(L<sub>2</sub>)<sub>2</sub>]

Color: brown; m.p.: >300 °C; yield (%): 73. Anal. Calc. for C<sub>32</sub>H<sub>54</sub>N<sub>4</sub>O<sub>10</sub>Si<sub>2</sub>Co (F.W: 770 g/mol): C, 49.92; H, 7.07; N, 7.28. Found: C, 49.84; H, 7.13; N, 7.14%. IR (KBr pellets,  $\nu_{\max}/\text{cm}^{-1}$ ): 3061  $\nu(\text{Ar–CH})$ , 2930–2871  $\nu(\text{Alif–CH})$ , 1608  $\nu(\text{C=N})$ , 1488–1405  $\nu(\text{C=C})$ , 1280  $\nu(\text{C–O})$ , 1122–1026  $\nu(\text{Si–O})$ , 521  $\nu(\text{Pd–N})$ , 464  $\nu(\text{Pd–O})$ .  $\mu_{\text{eff}} = 3.72$  [B.M.]. UV–vis ( $\lambda_{\max}$ , nm, \* = shoulder peak): 281, 289\*, 364, 478\* (in MeOH) and 273, 364, 472\* (in DMF).

### 2.2.7. For [Co(L<sub>3</sub>)<sub>2</sub>]

Color: dark brown; m.p.: >300 °C; yield (%): 76. Anal. Calc. for C<sub>32</sub>H<sub>54</sub>N<sub>4</sub>O<sub>8</sub>Si<sub>2</sub>Co (F.W: 738 g/mol): C, 52.09; H, 7.38; N, 7.59. Found: C, 52.12; H, 7.31; N, 7.54%. IR (KBr pellets,  $\nu_{\max}/\text{cm}^{-1}$ ): 3013  $\nu(\text{Ar–CH})$ , 2924–2865  $\nu(\text{Alif–CH})$ , 1614  $\nu(\text{C=N})$ , 1470–1391  $\nu(\text{C=C})$ , 1289  $\nu(\text{C–O})$ , 1138–1047  $\nu(\text{Si–O})$ , 514  $\nu(\text{Pd–N})$ , 464  $\nu(\text{Pd–O})$ .  $\mu_{\text{eff}} = 2.18$  [B.M.]. UV–vis ( $\lambda_{\max}$ , nm, \* = shoulder peak): 260, 394 (in MeOH) and 270, 395\* (in DMF).

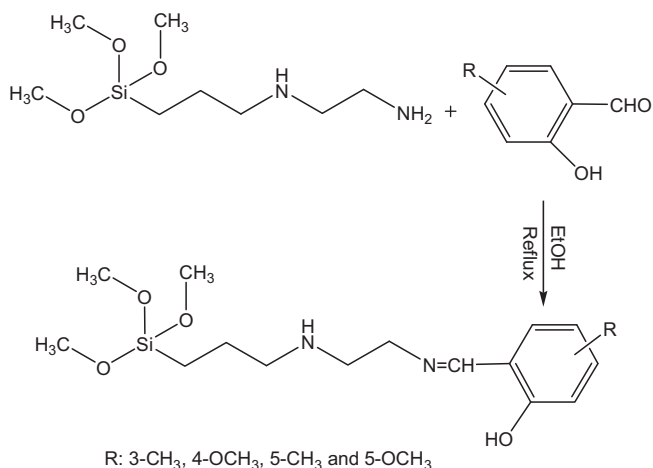
### 2.2.8. For [Co(L<sub>4</sub>)<sub>2</sub>]

Color: dark brown; m.p.: >300 °C; yield (%): 70. Anal. Calc. for C<sub>32</sub>H<sub>54</sub>N<sub>4</sub>O<sub>10</sub>Si<sub>2</sub>Co (F.W: 770 g/mol): C, 49.92; H, 7.07; N, 7.28. Found: C, 49.96; H, 7.02; N, 7.21%. IR (KBr pellets,  $\nu_{\max}/\text{cm}^{-1}$ ): 3025  $\nu(\text{Ar–CH})$ , 2925–2853  $\nu(\text{Alif–CH})$ , 1604  $\nu(\text{C=N})$ , 1470–1393  $\nu(\text{C=C})$ , 1286  $\nu(\text{C–O})$ , 1122–1034  $\nu(\text{Si–O})$ , 521  $\nu(\text{Pd–N})$ , 468  $\nu(\text{Pd–O})$ .  $\mu_{\text{eff}} = 2.26$  [B.M.]. UV–vis ( $\lambda_{\max}$ , nm, \* = shoulder peak): 257, 302\*, 409 (in MeOH) and 274, 294, 305, 412 (in DMF).

## 2.3. Reactions of carbon dioxide and epoxides

All the catalytic reaction experiments were performed in a stainless steel pressure reactor of 50 mL with a stirrer. The reactor was charged with complexes ( $4.5 \times 10^{-5}$  mol), epoxide ( $4.5 \times 10^{-2}$  mol), DMAP (11 mg,  $9.0 \times 10^{-5}$  mol). The reaction vessel was placed under a constant pressure of carbon dioxide for 2 min to allow the system to equilibrate and CO<sub>2</sub> was charged into the autoclave with desired pressure then heated to the desired temperature. The pressure was kept constant during the reaction. The vessel was then cooled to 5–10 °C in ice bath after the expiration of the desired time of reaction. The pressure was released, then, the excess gases were vented.

For recycling studies, the catalyst [Pd(L<sub>3</sub>)<sub>2</sub>] and base(DMAP) were separated from the reaction mixture by vacuum distillation at



Scheme 1. Synthesis route of ligands.

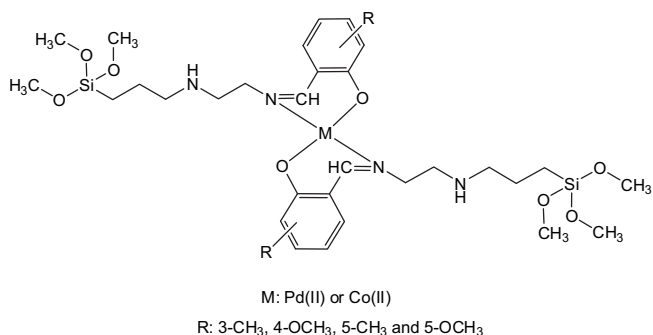
80 °C. Reuseability of  $[\text{Pd}(\text{L}_3)_2]/\text{DMAP}$  catalytic system was performed using propylene oxide as substrate which is available for many applications and easier to separate propylene carbonate from the reaction mixture by vacuum distillation. After distillation of the propylene carbonate and propylene oxide, DMAP and  $[\text{Pd}(\text{L}_3)_2]$  stayed in the reaction pot. Adding the same amount of PO, the second reuse was performed. The yields of epoxides to corresponding cyclic carbonates were determined by comparing the ratio of product to substrate in the  $^1\text{H}$  NMR spectrum of an aliquot of the reaction mixture.

### 3. Results and discussion

#### 3.1. Synthesis and spectral properties

The chemical structures of silicon-containing ligands used in this work and the synthetic paths to the Pd(II) and Co(II) metal complexes created with these ligands are illustrated in Schemes 1 and 2. The compounds are yellow ligands, green or dark green Pd(II) metal complexes and brown or dark brown Co(II) metal complexes solids at room temperature. Ligands ( $\text{L}_1\text{H}$ ), ( $\text{L}_2\text{H}$ ), ( $\text{L}_3\text{H}$ ), and ( $\text{L}_4\text{H}$ ) were prepared by condensation between different salicylaldehyde and *N*-(3-(trimethoxysilyl)propyl)-ethylenediamine using the general method described for the preparation of salicylaldimine ligands [23,24]. Its characterization data (see Experimental section) agreed with the proposed formulae.

Treatment of 2:1 molar ratio amounts of ligands and  $\text{Pd}(\text{AcO})_2$  or  $\text{Co}(\text{AcO})_2 \cdot 4\text{H}_2\text{O}$  in refluxing methanol for 8 h, followed by the removal of small amounts other residues, produced  $[\text{M}(\text{L}_n)_2]$



Scheme 2. The proposed structure for the Pd(II) and Co(II) complexes.

( $\text{M} = \text{Pd}$  or  $\text{Co}$ ,  $n = 1-4$ ) (Scheme 2). The elemental analyses and other analytical data were consistent with the proposed formulae. The Pd(II) and Co(II) metal complexes were observed to precipitate from solution during the reaction as orange-brown solids for Co(II) metal complexes and as pale-green solids for Pd(II) metal complexes, which were purified by recrystallisation. All metal complexes were found to be stable in the solid state at room temperature for months. The metal complexes were also fairly stable in different solution for days even in the absence of nitrogen, showing no visible signs of decomposition.

The  $^1\text{H}$  NMR spectral results obtained for ligands ( $\text{L}_1\text{H}$ ,  $\text{L}_2\text{H}$ ,  $\text{L}_3\text{H}$  and  $\text{L}_4\text{H}$ ) and their mononuclear Pd(II) metal complexes in  $\text{DMSO}-d_6$  did not give any signal corresponding to amine group and different salicylaldehyde protons. The ligands and their mononuclear Pd(II) metal complexes give well-defined  $^1\text{H}$  NMR spectra, which permit unambiguous identification and assessment of purity. The proton chemical shifts are assigned with the influence of steric, inductive and conjugative effects and compared with those of similar compounds [25–27]. The mononuclear Pd(II) metal complexes of different ligands are in different magnetic environments. The spectrum of Pd(II) complexes were compared with that of the parent salicylaldimine ligands. The OH signal found between 13.66 and 12.68 ppm as singlet in the spectrum of the salicylaldimine ligands due to intramolecular  $\text{OH} \cdots \text{N}$  hydrogen bonding completely disappeared in the spectrum of the Pd(II) metal complexes. These signals are  $\text{D}_2\text{O}$  exchangeable. This result indicates the involvement of the OH group in chelation with Pd(II) through displacement of *ortho* hydroxyl proton [28,29]. The singlets corresponding to azomethine group were observed between 8.60 and 8.42 ppm for ligands. The azomethine group has undergone a downfield shift of 0.47–0.29 ppm indicating the participation of azomethine nitrogen in coordination [30]. The peaks at range 7.25–6.77 ppm for ( $\text{L}_1\text{H}$ ), at range 7.27–6.37 ppm for ( $\text{L}_2\text{H}$ ), at range 7.19–6.73 ppm for ( $\text{L}_3\text{H}$ ) and at range 7.00–6.77 ppm for ( $\text{L}_4\text{H}$ ) are assignable to the protons of  $\text{Ar}-\text{CH}$  as singlet, doublet or multiplet peaks. These peaks are observed at range 7.71–6.19 ppm for all Pd(II) metal complexes, as singlet, doublet or multiplet peaks. The other results of the ligands and their Pd(II) metal complexes are given in Experimental section.

The infrared spectra of ligands ( $\text{L}_1\text{H}$ ,  $\text{L}_2\text{H}$ ,  $\text{L}_3\text{H}$  and  $\text{L}_4\text{H}$ ) and their Pd(II) and Co(II) metal complexes have been studied order to characterize their structures. The FT-IR spectra of all compounds were carried out in the  $4000-400\text{ cm}^{-1}$  range. The characteristic infrared spectrum data are given in Experimental section. The  $\nu$  (O–H) vibration of the free ligands is observed in the range  $3546-2504\text{ cm}^{-1}$ . The occurrence of this band at such a relatively low wavenumber is characteristic of these ligands and is an indication of fairly extensive hydrogen bonding [31]. In the FT-IR spectra of Pd(II) and Co(II) metal complexes, this band does not appear as expected. Characteristic absorptions in the FT-IR spectra of ligands and their Pd(II) and Co(II) metal complexes are represented by stretching vibrations of the  $\nu(\text{C}=\text{N})$  group of ligands between  $1632$  and  $1631\text{ cm}^{-1}$ . The low frequency shift of the  $\nu(\text{C}=\text{N})$  stretch (in between  $1616$  and  $1602\text{ cm}^{-1}$  for Pd(II) and  $1614$  and  $1604\text{ cm}^{-1}$  for Co(II) complexes), in comparison with the free ligands, is consistent with N-coordination of Pd(II) and Co(II) ions to the azomethine ligands [32,33]. The coordination of the salicylaldimine ligands to the Pd(II) or Co(II) centre through the azomethine nitrogen atom is expected to reduce the electron density in the azomethine link and lower the  $\nu(\text{C}=\text{N})$  absorption frequency. Coordination is further confirmed by shift in the  $\nu(\text{C}-\text{O})$  stretching vibration of the phenoxy group from the region  $1280-1264\text{ cm}^{-1}$  to a higher frequency range for Pd(II) and Co(II) metal complexes which indicates M–O coordination [31,34,35]. The coordination of the azomethine nitrogen and phenolic oxygen is

further supported by the appearance of two peaks at 521–512  $\text{cm}^{-1}$  for  $\nu(\text{M}-\text{N})$  and 468–462  $\text{cm}^{-1}$  for  $\nu(\text{M}-\text{O})$ , due to stretching vibrations that are not observed in the infrared spectra of the ligands [36]. Thus, it is clear that the ligands are bonded to the palladium and cobalt metal ion in an  $\text{N}_2\text{O}_2$  fashion through the deprotonated phenolate oxygen, and azomethine nitrogen. This peak is not observed in the free ligands. These results agree with the expected structures. The results show that Pd(II) and Co(II) complexes indicate deprotonation and coordination of the phenolic OH group. It also confirms that nitrogen atom of the azomethine group contributes to the complexation.

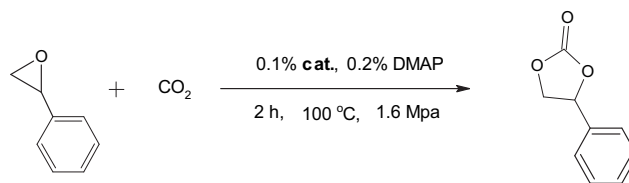
Electronic spectra of ligands ( $\text{L}_1\text{H}$ ,  $\text{L}_2\text{H}$ ,  $\text{L}_3\text{H}$  and  $\text{L}_4\text{H}$ ) and their mononuclear Pd(II) and Co(II) metal complexes have been recorded in the 1100–200 nm range in EtOH, MeOH, and DMF (for ligands) and in MeOH and DMF (for metal complexes) solutions and their corresponding data are given in Experimental section. The absorption bands in the visible region can be safely assigned to spin-allowed MLCT transitions, whereas the absorption bands in the ultraviolet region are assigned to LC transitions. The electronic spectra of the free ligands in EtOH, MeOH, and DMF showed strong absorption bands in the UV–vis region (301–456 nm), attributed to the  $\pi \rightarrow \pi^*$  or  $n \rightarrow \pi^*$  transitions. Also, the free ligands exhibited a UV bands attributed to the  $n \rightarrow \pi^*$  or  $n \rightarrow \sigma^*$  transitions [25,26]. The spectra of the Pd(II) and Co(II) metal complexes showed modifications with respect to the position and intensity of the characteristic bands to the free ligands as compared. They also new bands which were attributed to the formed metal complexes [37]. The absorption bands in the range of 394–472 nm were attributed to the  $d \rightarrow \pi^*$  charge-transfer transitions, which are overlapping with the  $\pi \rightarrow \pi^*$  or  $n \rightarrow \pi^*$  transitions of the ligands. The spectrum of the free ligands was compared with the spectra of the metal complexes, a new broad but weak peak is observed at range 514–639 nm in different solvents for Pd(II) and Co(II) metal complexes, which can be assigned to the metal-ligand charge-transfer (MLCT) absorption between the central Pd(II) and Co(II) ion and ligands. These modifications of the shifts and intensity of the absorption bands, confirmed the coordination of the ligand to the Pd(II) or Co(II) central metallic ion. A square planar geometry for Pd(II) and tetragonal geometry for Co(II) complexes with four donor atoms ( $\text{N}_2\text{O}_2$ ) in the same plan was proposed for the metal complexes in solid state [38].

Magnetic susceptibility measurements provide sufficient data to characterize the structure of the metal complexes. Magnetic moments measurements of Co(II) metal complexes are carried out in the solid state at room temperature and results are given in Experimental section. The magnetic moments of the Co(II) complexes are 2.24 B.M. (low-spin) for  $[\text{Co}(\text{L}_1)_2]$ , 3.72 B.M. (high-spin) for  $[\text{Co}(\text{L}_2)_2]$ , 2.18 B.M. (low-spin) for  $[\text{Co}(\text{L}_3)_2]$  and 2.26 B.M. (low-spin) for  $[\text{Co}(\text{L}_4)_2]$ , respectively which suggests tetragonal geometry for Co(II) metal complexes. Magnetic moments measurements of Pd(II) metal complexes carried out at 25 °C show that all Pd(II) complexes are diamagnetic, indicating the low-spin ( $S = 0$ ) square planar  $d^8$ -systems, as expected.

### 3.2. Catalytic properties

The coupling of carbon dioxide and epoxides catalyzed by Pd(II) and Co(II) (Scheme 2) was investigated under different reaction conditions. The results were shown in Tables 1 and 2. The yields of epoxides to corresponding cyclic carbonates were determined by comparing the ratio of product to substrate in the  $^1\text{H}$  NMR spectrum of an aliquot of the reaction mixture (Fig. 1). It can be seen that the catalysts of  $[\text{Pd}(\text{L}_3)_2]$  and  $[\text{Co}(\text{L}_3)_2]$  have more effective activities than the other Pd(II) and Co(II) metal complexes for the formation of cyclic organic carbonates from carbon dioxide (Fig. 2).

**Table 1**  
Synthesis of styrene carbonate from styrene oxide and  $\text{CO}_2$  catalyzed by synthesized complexes.



Entries	Catalysts	Yield <sup>a</sup>	TON <sup>b</sup>	TOF <sup>c</sup> ( $\text{h}^{-1}$ )
1	$[\text{Pd}(\text{L}_1)_2]$	74	740	370
2	$[\text{Pd}(\text{L}_2)_2]$	81	810	405
3	$[\text{Pd}(\text{L}_3)_2]$	82	820	410
4	$[\text{Pd}(\text{L}_4)_2]$	79	790	395
5	$[\text{Co}(\text{L}_1)_2]$	58	580	290
6	$[\text{Co}(\text{L}_2)_2]$	47	470	235
7	$[\text{Co}(\text{L}_3)_2]$	81	810	405
8	$[\text{Co}(\text{L}_4)_2]$	42	420	210

<sup>a</sup> Yield of styrene oxide to styrene carbonate was determined by comparing the ratio of product to substrate in the  $^1\text{H}$  NMR spectrum of an aliquot of the reaction mixture (see Fig. 2).

<sup>b</sup> Moles of cyclic carbonate produced per mole of catalyst.

<sup>c</sup> The rate is expressed in terms of the turnover frequency (TOF (mole of product (mole of catalyst  $\text{h}^{-1}$ )) = turnovers/h).

The results shown that the Pd(II) and Co(II) complexes bearing 5-methyl substituent on the aryl ring ( $[\text{M}(\text{L}_3)_2]$ ) are more efficient than the other Pd(II) and Co(II) metal complexes. The presence of solvent such as dichloromethane did not use for all catalytic run due to redundant according to previous study [39]. The catalyst  $[\text{Pd}(\text{L}_3)_2]$  shows low activity (15% yield) without addition of DMAP that can enhance the Lewis acidity of  $\text{Pd}^{2+}$ . While using only the DMAP as catalyst without absence of metal species gave only 5% conversion at the same catalytic conditions. As a result of this conclusion it

**Table 2**  
Coupling of  $\text{CO}_2$  and various epoxides catalyzed by complex  $[\text{Pd}(\text{L}_3)_2]$ .

Entries	Product	Yield (%)	Selectivity (%)	TON	TOF ( $\text{h}^{-1}$ )
1		82	99	820	410
2		74	99	740	370
3		99	98	990	495
4		69	97	690	345

Reaction conditions: **6** ( $4.5 \times 10^{-5}$  mol), DMAP ( $9 \times 10^{-5}$  mol), epoxide ( $4.5 \times 10^{-2}$  mol),  $\text{CO}_2$  (1.6 MPa), 100 °C, 2 h.

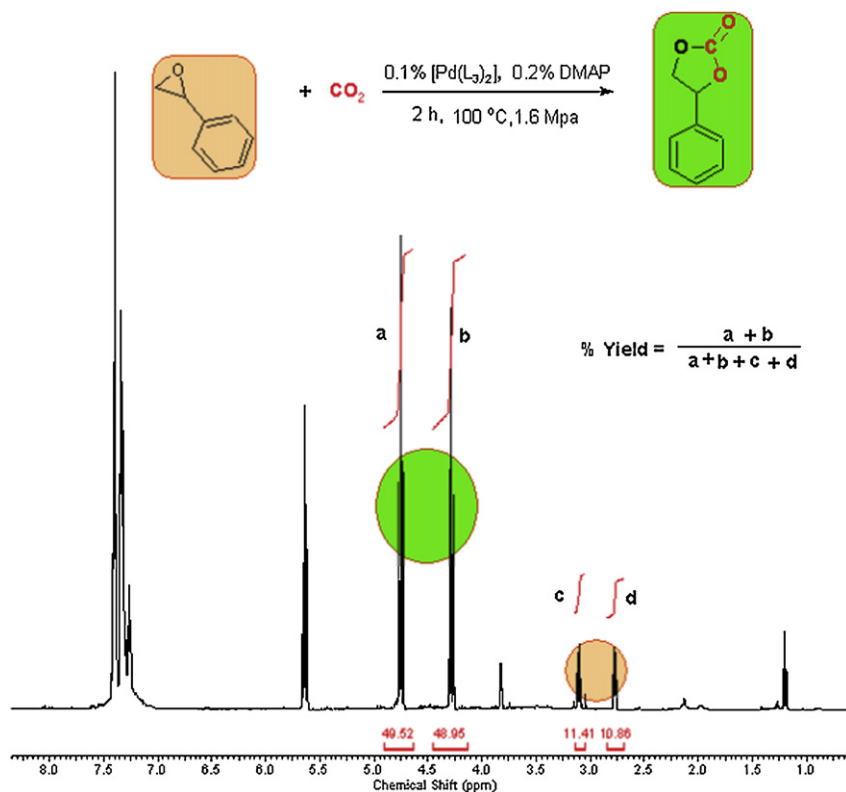


Fig. 1. A typical  $^1\text{H}$  NMR spectra of the reaction mixture (Table 1, entry 3).

can be understood that metal catalyst must be used with a Lewis base such as DMAP. A comparative study with DMAP and  $\text{NEt}_3$  was investigated. DMAP is more active base with 82% yield, the yield is decreased to 23% when  $\text{NEt}_3$  was replaced as base.

Regarding the reaction mechanism we envisioned the occurrence of a similar pathway to the one proposed previously [40], i.e. activation of the epoxide by a Lewis acid and attacks of Lewis base (DMAP) to the sterically less hindered carbon atom to open the epoxide ring. The generated oxy anion species then reacts with  $\text{CO}_2$  to give the cyclic carbonate. Lewis base such as DMAP,  $\text{NEt}_3$  and DBU is required as co-catalyst for the catalytic cycle. The catalytic system is co-catalyzed by a Lewis base amine and Lewis acid metal centre. The Lewis base and Lewis acid work together to open the epoxy ring and then react with  $\text{CO}_2$  to give the corresponding cyclic carbonate via a ring opening and recyclization process [41–43].

When the reaction temperature and the time rise, the yield of this reaction was augmented by using catalyst  $[\text{Pd}(\text{L}_3)_2]/\text{DMAP}$  (Fig. 3) [39,44]. Meanwhile the electron-withdrawing groups at the 2-position of the epoxide activated the substrate, while electron donating substituents deactivate the epoxide (see Table 2). Epichlorohydrin was found to be the most reactive epoxide, while propylene epoxide exhibited the lowest activity of the epoxides surveyed.

The reaction conditions such as reaction time, temperature and  $\text{CO}_2$  pressure were shown to have an influence on the catalytic activity of transformation of SO to its related cyclic carbonate using  $[\text{Pd}(\text{L}_3)_2]$  as catalyst (see Fig. 3). The influence of temperature on the yield of styrene carbonate (SC) was investigated at  $\text{CO}_2$  pressures of 1.6 MPa. The yield of SC strongly depended on reaction temperature (Fig. 3c). In the lower temperature range, the yield increased with increasing temperature. However, the yield decreased slightly in

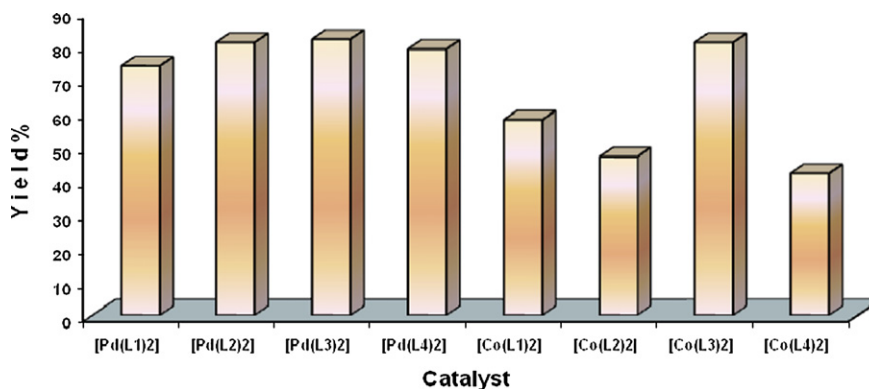


Fig. 2. The comparison of metal catalysts for the formation of styrene oxide to corresponding cyclic carbonate (styrene carbonate) at the same catalytic conditions.

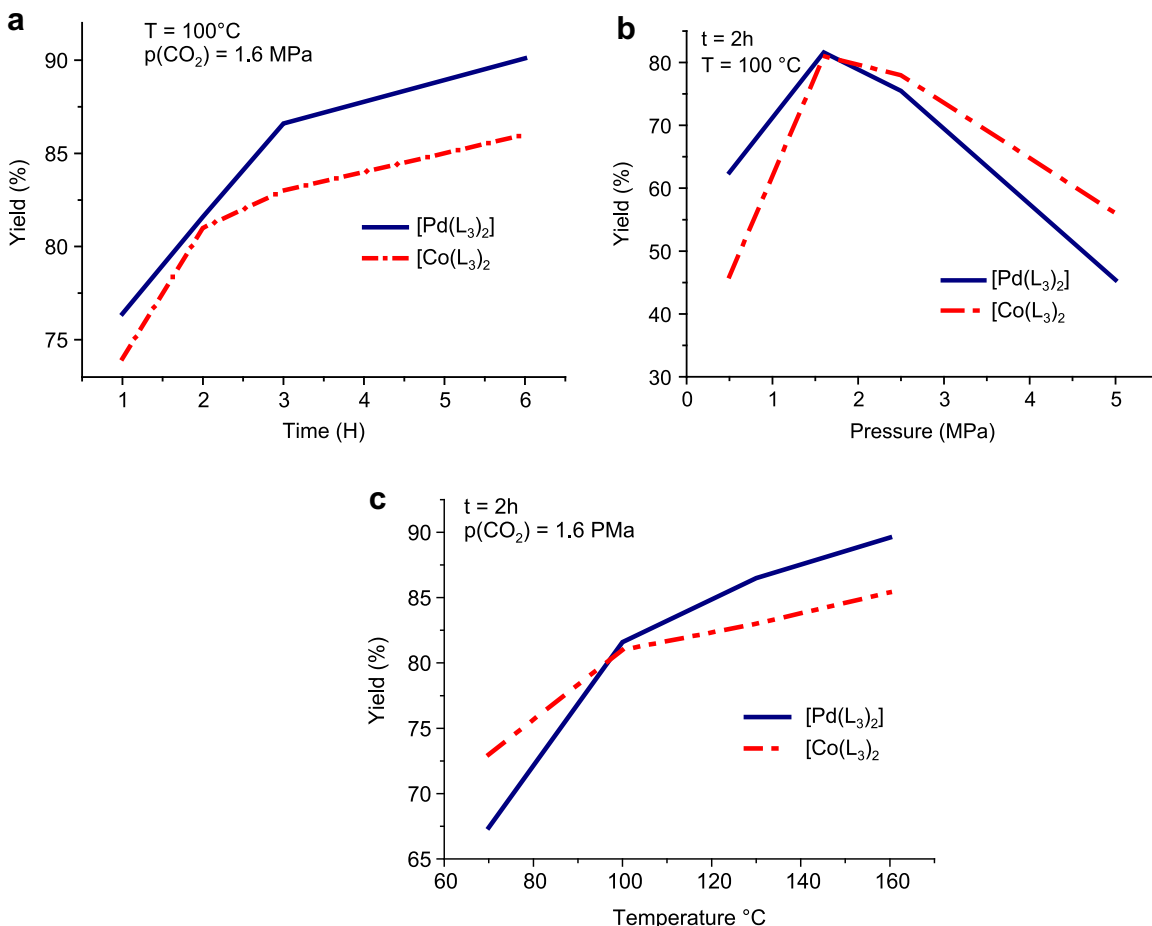


Fig. 3. Conversion of styrene oxide as a function of time (a), pressure (b) and temperature (c) with active complexes.

the high-temperature region. Time is also effective parameter of the conversion. SO reached 94% yield within 6 h, at 100 °C (Fig. 3a). Fig. 4b shows the dependence of SC yield on pressure at 100 °C with a reaction time of 2 h. An increase in pressure resulted in an increase in the SC yield in the low-pressure region up to 1.8 MPa and a decrease of the yield in the high-pressure region. A similar effect was reported by Darensbourg et al. [45], catalytic transformation of CO<sub>2</sub> to polycarbonate increased with increasing the pressure, but the value of TOF was decreased. The main reason for this phenomenon was reported by Han et al. [44] as phase

behaviour of the substrates and CO<sub>2</sub>. In all catalytic runs, the selectivity for the chemical fixation of CO<sub>2</sub> into cyclic carbonate form is over 98%. One of the active catalyst [Pd(L<sub>3</sub>)<sub>2</sub>] is reused more than eight times with a minimal loss of its original catalytic activity (Fig. 4). According to Fig. 4, we optimized the best fit catalytic conditions (1.8 MPa CO<sub>2</sub>, 110 °C and 2 h) for reuse studies. During the catalytic recycling of [Pd(L<sub>3</sub>)<sub>2</sub>]/DMAP, there was a small reduction of the propylene carbonate since, at the end of the eighth cycle the value was, respectively, 14% lower than initial value (Fig. 4).

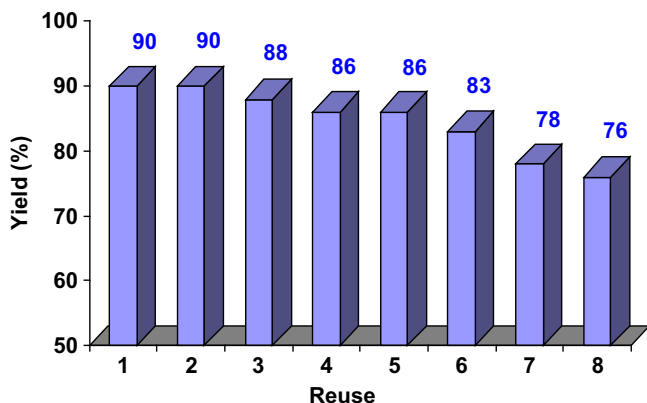


Fig. 4. Recycling studies of propylene oxide by [Pd(L<sub>3</sub>)<sub>2</sub>] catalyst.

#### 4. Conclusions

A new series of metal complexes of salicyladimine ligands with Pd(II) and Co(II) have been prepared and characterized by different techniques. The new complexes, synthesized in good yields, generate an active and useful catalyst for cycloaddition of CO<sub>2</sub> to epoxides in good to excellent yields. The electron donating substituent on the *p*-position of aryl ring of the ligand system accelerates the chemical fixation of CO<sub>2</sub> into cyclic carbonates. The active catalyst [Pd(L<sub>3</sub>)<sub>2</sub>] was reused more than eight times with a minimal loss of its original catalytic activity.

#### Acknowledgment

This work has been supported by the Research Fund of Harran University (Sanliurfa, Turkey).

## References

- [1] H. Arakawa, M. Aresta, J.N. Armor, M.A. Barteau, E.J. Beckman, A.T. Bell, J.E. Bercaw, C. Creutz, E. Dinjus, D.A. Dixon, K. Domen, D.L. DuBois, J. Eckert, E. Fujita, D.H. Gibson, W.A. Goddard, D.W. Goodman, J. Keller, G.J. Kubas, H.H. Kung, J.E. Lyons, L.E. Manzer, T.J. Marks, K. Morokuma, K.M. Nicholas, R. Periana, L. Que, J. Rostrup-Nielson, W.M.H. Sachtler, L.D. Schmidt, A. Sen, G.A. Somorjai, P.C. Stair, B.R. Stults, W. Tumas, *Chem. Rev.* 101 (2001) 953–996.
- [2] T. Sakakura, J.C. Choi, H. Yasuda, *Chem. Rev.* 107 (2007) 2365–2387.
- [3] J. Wang, J. Wu, N. Tang, *Inorg. Chem. Commun.* 10 (2007) 1493–1495.
- [4] D. Braunstein, D. Matt, D. Nobel, *Chem. Rev.* 88 (1988) 747–764.
- [5] K.C. Nicolaou, Z. Yang, J.J. Liu, H. Ueno, P.G. Nantermet, R.K. Guy, C.F. Claiborne, H. Renaud, E.A. Couladouros, K. Paulvannanand, E.J. Sprensen, *Nature* 367 (1994) 630–634.
- [6] T. Takata, Y. Furusho, K.I. Murakawa, T. Endo, H. Matsuoka, T. Hirasa, J. Matsuo, M. Sisido, *J. Am. Chem. Soc.* 120 (1998) 4530–4531.
- [7] H.T. Chang, K.B. Sharpless, *Tetrahedron Lett.* 37 (1996) 3219–3222.
- [8] A.G. Shaikh, *Chem. Rev.* 96 (3) (1996) 951–976.
- [9] J.H. Clements, *Ind. Eng. Chem. Res.* 42 (4) (2003) 663–676.
- [10] G. Rokicki, *Prog. Polym. Sci.* 25 (2000) 259–342.
- [11] D.J. Darensbourg, M.W. Holtcamp, *Coord. Chem. Rev.* 153 (1996) 155–174.
- [12] S. Inoue, *CHEMTECH* 6 (1976) 588–594.
- [13] W. Kuran, *Prog. Polym. Sci.* 23 (1998) 919–992.
- [14] D.J. Darensbourg, P. Bottarelli, J.R. Andreatta, *Macromolecules* 40 (2007) 7727–7729.
- [15] D.J. Darensbourg, R.M. Mackiewicz, A.L. Phelps, D.R. Billodeaux, *Acc. Chem. Res.* 37 (2004) 836–844.
- [16] R.L. Paddock, S.T. Nguyen, *J. Am. Chem. Soc.* 123 (2001) 11498–11499.
- [17] R. Eberhardt, M. Allmendinger, B. Rieger, *Macromol. Rapid Commun.* 24 (2003) 194–196.
- [18] B. Li, R. Zhang, X.B. Lu, *Macromolecules* 40 (2007) 2303–2307.
- [19] G.W. Coates, D.R. Moore, *Angew. Chem., Int. Ed.* 43 (2004) 6618–6639.
- [20] D.J. Darensbourg, M. Ulusoy, O. Karronnirun, R.R. Poland, J.H. Reibenspies, B. Cetinkaya, *Macromolecules* 42 (2009) 6992–6998.
- [21] A. Orejon, A.M. Masdeu-Bulto, P. Salagre, S. Castillon, C. Claver, A. Padilla, B. Almena, F.L. Serrano, *Ind. Eng. Chem. Res.* 47 (2008) 8032–8036.
- [22] A. Earnshaw, *Introduction to Magnetochemistry*. Academic Press, London, 1968, p. 4.
- [23] A. Kilic, E. Tas, B. Devenci, I. Yilmaz, *Polyhedron* 26 (2007) 4009–4018.
- [24] E. Tas, A. Kilic, N. Konak, I. Yilmaz, *Polyhedron* 27 (2008) 1024–1032.
- [25] L. Tan, Y. Xiao, X. Liu, S. Zhang, *Spectrochim. Acta, Part A* 73 (5) (2009) 858–864.
- [26] A. Ambroise, B.G. Maiya, *Inorg. Chem.* 39 (2000) 4256–4263.
- [27] B. Onfelt, P. Lincoln, B. Norden, *J. Am. Chem. Soc.* 121 (1999) 10846–10847.
- [28] E. Tas, A. Kilic, M. Durgun, I. Yilmaz, I. Ozdemir, N. Gurbuz, *J. Organomet. Chem.* 694 (2009) 446–454.
- [29] M.A. Neelakantan, S.S. Marriappan, J. Dharmaraja, T. Jeyakumar, K. Muthukumar, *Spectrochim. Acta, Part A* 71 (2) (2008) 628–635.
- [30] K.B. Gudasi, M.S. Patil, R.S. Vadavi, R.V. Shenoy, S.A. Patil, *Trans. Met. Chem.* 31 (2006) 986–991.
- [31] J.L. van Wyk, S. Mapolie, A. Lennartson, M. Hakkansson, S. Jagner, *Inorg. Chim. Acta* 361 (2008) 2094–2100.
- [32] O.N. Kadkin, J. An, H. Han, Y.G. Galyametdinov, *Eur. J. Inorg. Chem.* 10 (2008) 1682–1688.
- [33] A. Kilic, I. Yilmaz, M. Ulusoy, E. Tas, *Appl. Organomet. Chem.* 22 (2008) 494–502.
- [34] E. Schön, D.A. Plattner, P. Chen, *Inorg. Chem.* 43 (2004) 3164–3169.
- [35] E. Tas, M. Aslanoglu, M. Ulusoy, H. Temel, *J. Coord. Chem.* 57 (8) (2004) 677–684.
- [36] E. Tas, I.H. Onal, I. Yilmaz, A. Kilic, M. Durgun, *J. Mol. Struct.* 927 (2009) 69–77.
- [37] A. Pui, C. Policar, J.P. Mahy, *Inorg. Chim. Acta* 360 (2007) 2139–2144.
- [38] A.B.P. Lever, *Inorganic Electronic Spectroscopy*, second ed. Elsevier, London, 1992.
- [39] M. Ulusoy, E. Cetinkaya, B. Cetinkaya, *Appl. Organomet. Chem.* 23 (2009) 68–74.
- [40] Z. Bu, G. Qin, S. Cao, *J. Mol. Catal. A* 277 (1–2) (2007) 35–39.
- [41] Y.M. Shen, W.L. Duan, M. Shi, *J. Org. Chem.* 68 (2003) 1559–1562.
- [42] L.D. Field, W.J. Shaw, P. Turner, *Chem. Commun.* (2002) 46–47.
- [43] D.H. Gibson, *Chem. Rev.* 96 (1996) 2063–2095.
- [44] Y. Xie, Z. Zhang, T. Jiang, J. He, B. Han, T. Wu, K. Ding, *Angew. Chem., Int. Ed.* 46 (2007) 7255–7258.
- [45] D.J. Darensbourg, R.M. Mackiewicz, D.R. Billodeaux, *Organometallics* 24 (2005) 144–148.